

Figure S1

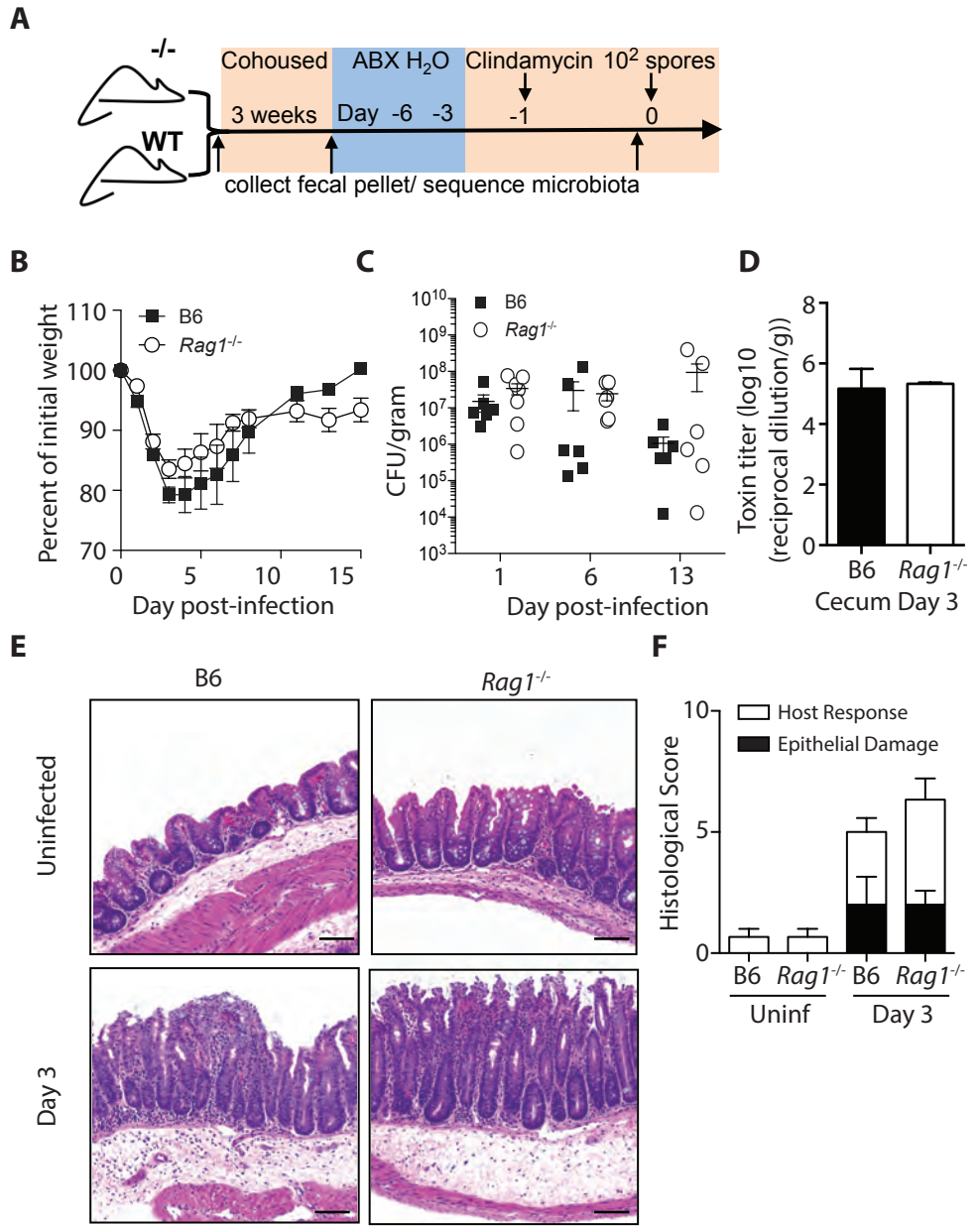


Figure S1. The innate immune response is sufficient for acute recovery following *C. difficile* infection. Related to Figure 1. C57BL/6 and *Rag1*^{-/-} mice were infected with 200 spores of *C. difficile* (VPI 10463 strain) following antibiotic pretreatment and were assessed for **(A)** Schematic for co-housing, antibiotic pretreatment and *C. difficile* infection. **(B)** weight loss and recovery following infection. **(C)** *C. difficile* burden in fecal pellets. **(D)** Toxin levels present in the cecal content at day 3 post-infection. **(E)** Representative H&E stained cecal sections from antibiotic-treated, uninfected and day 3 infected C57BL/6 or *Rag1*^{-/-} mice. Scale bar = 100µm. **(F)** Pathology score of histological tissue sections based on cellular infiltration/edema (host response), and epithelial layer degeneration. Data representative of 4 independent experiments; n= 4-5 mice per group.

Figure S2

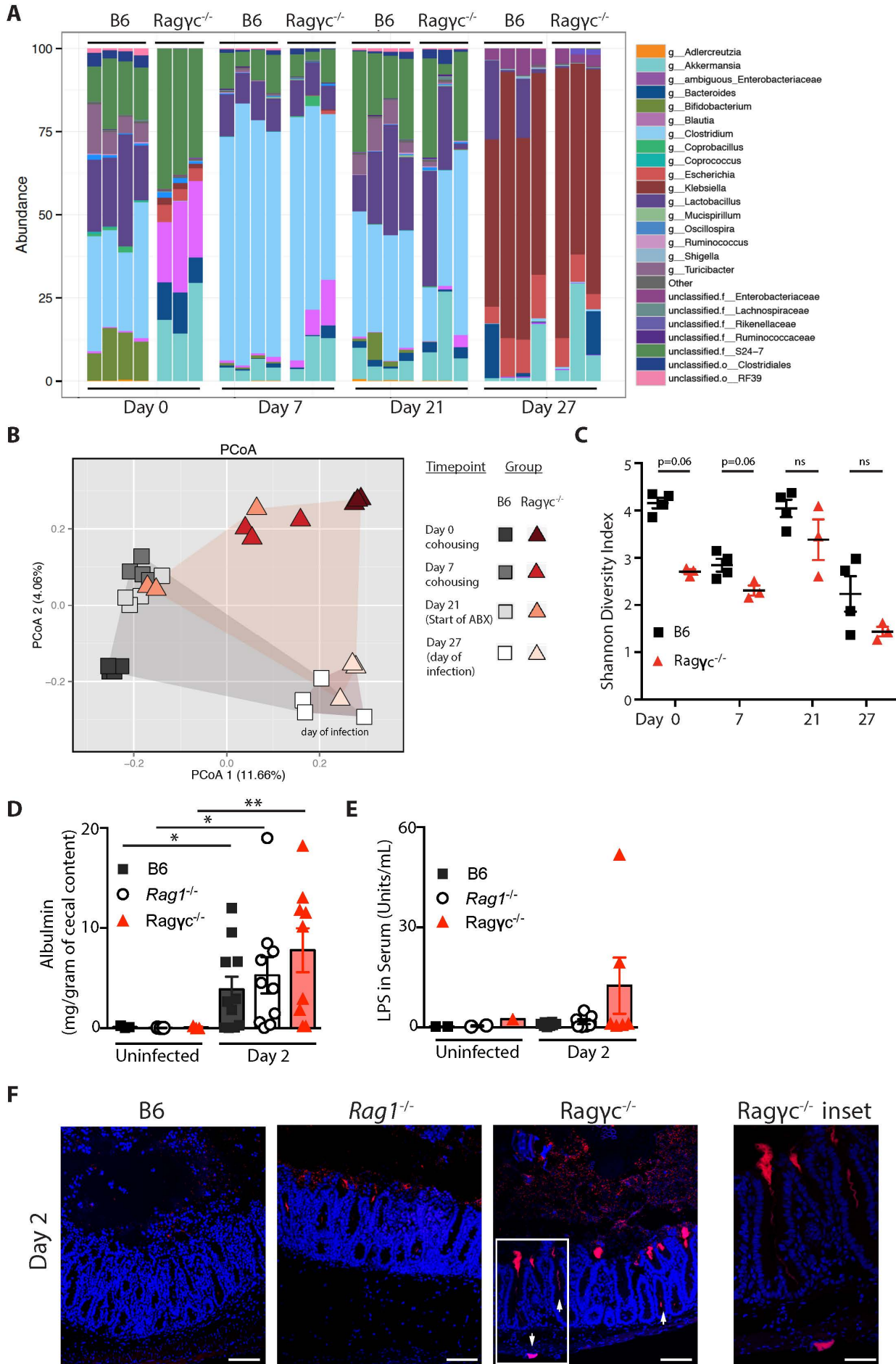


Figure S2. Cohoused Rag γ C^{-/-} mice equilibrate their intestinal microbiota prior to infection and have indication of increased bacterial translocation following infection. Related to Figure 1. Fecal pellets were collected from C57BL/6 and Rag γ C^{-/-} mice at the start of cohousing, day 7 of cohousing, day 21 of cohousing (start of antibiotic treatment), and day 27 of cohousing (day of *C. difficile* infection). Bacterial DNA was isolated from pellets and sequenced using an Illumina MiSeq platform. **(A)** Genus level abundance of intestinal bacterial communities. Each bar represents an individual mouse. **(B)** Principal component analysis of intestinal bacterial communities. **(C)** Intestinal bacterial diversity of C57BL/6 and Rag γ C^{-/-} mice as calculated by the Shannon Diversity Index. **(D)** Albumin concentration in the cecal content and **(E)** serum LPS concentration of uninfected and day 2 infected C57BL/6, Rag1^{-/-}, Rag γ C^{-/-} mice. **(F)** Bacterial FISH staining of cecal sections from day 2 infected C57BL/6, Rag1^{-/-}, Rag γ C^{-/-} mice (blue - Hoescht, red -universal 16S bacteria probe). Arrows point to bloom of bacteria in intestinal crypt. Scale bar = 100 μ m; inset = 50 μ m. *p<0.05, **p<0.01. Data shown are mean \pm SEM.

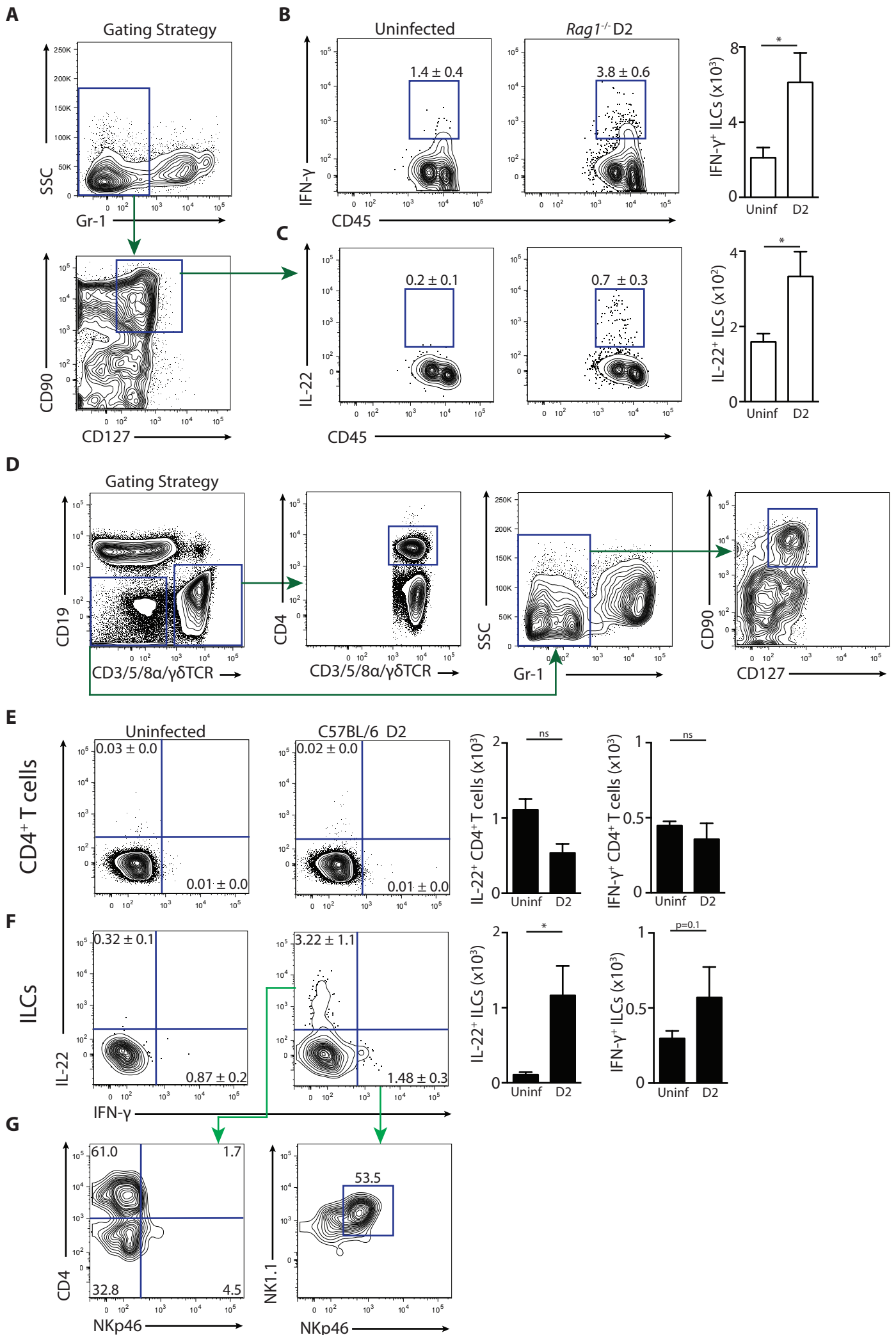


Figure S3. Induction of IL-22 and IFN- γ expressing ILCs in the mesenteric lymph nodes of *Rag1*^{-/-} or C57BL/6 mice following *C. difficile* infection. Related to Figure 3. Cells isolated from the mLN of uninfected or day 2 infected *Rag1*^{-/-} or C57BL/6 mice were incubated in media in the presence of BFA and assessed for IL-22 and IFN- γ production. **(A)** Gating strategy used to identify CD90⁺, CD127⁺ ILCs from *Rag1*^{-/-} mice. Initial FACS plot gated on live, CD45⁺ cells. Frequency and number of **(B)** IFN- γ ⁺ or **(C)** IL-22⁺ ILCs in *Rag1*^{-/-} mice. Data representative of 3 independent experiments; n=4-5 mice per group. **(D)** Gating strategy used to identify CD4⁺ T cells and CD90⁺, CD127⁺ ILCs from C57BL/6 mice. Initial FACS plot gated on live, CD45⁺ cells. **(E)** Frequency and number of IL-22⁺ or IFN- γ ⁺ CD4⁺ T cells. **(F)** Frequency and number of IL-22⁺ or IFN- γ ⁺ ILCs **(G)** Expression of NKp46, CD4 or NK1.1 on cytokine positive ILCs from day 2 infected C57BL/6 mice. Data representative of 3 independent experiments; n=3-5 mice per group. *p<0.05. Data shown are mean \pm SEM.

Figure S4

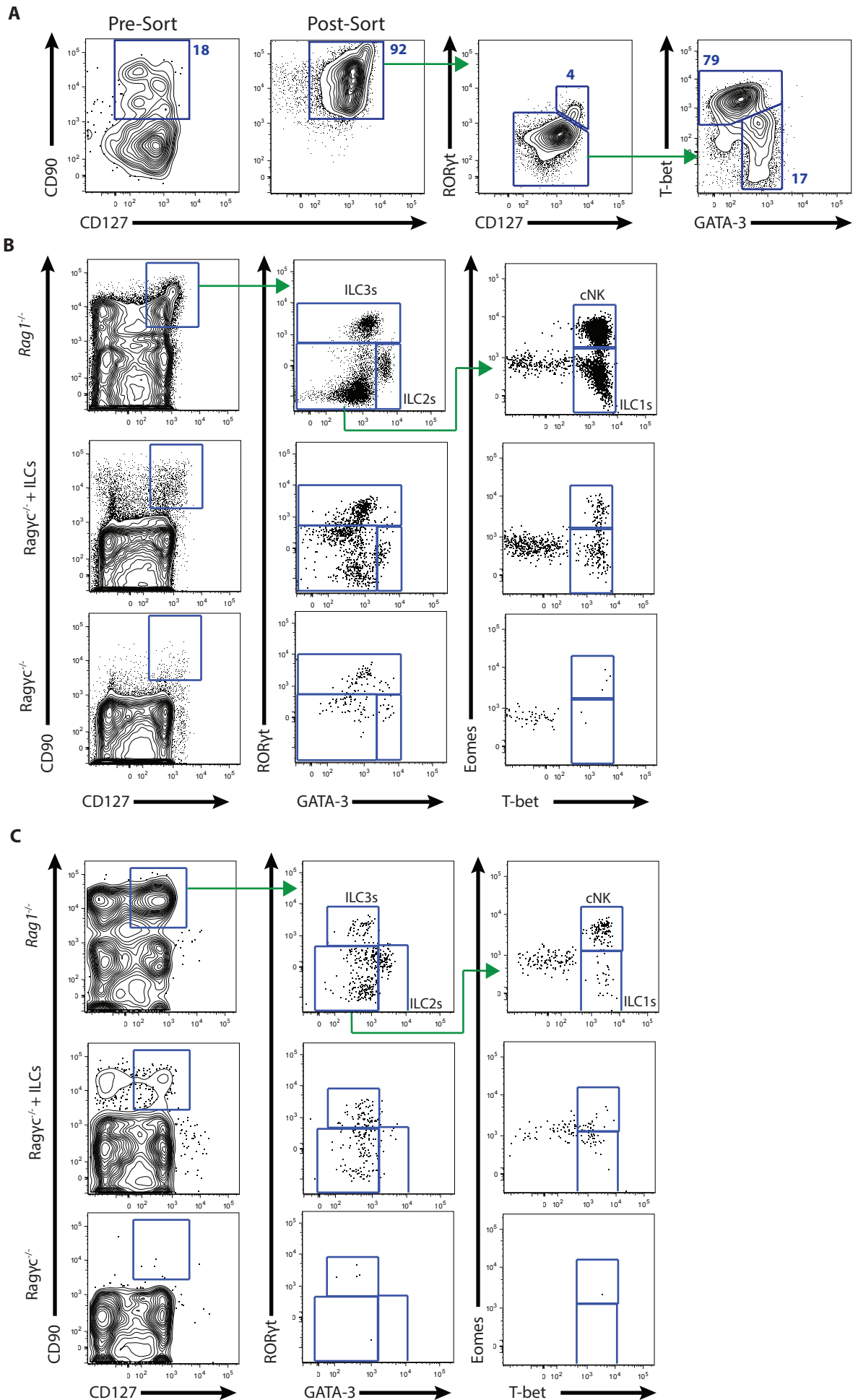
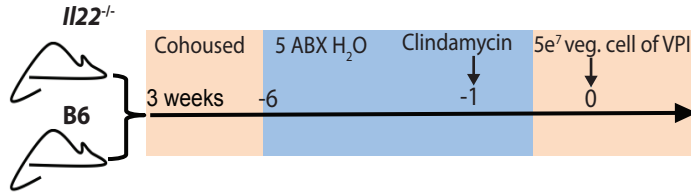


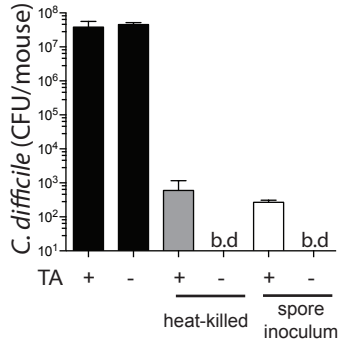
Figure S4. ILC adoptive transfer into $Rag\gamma c^{-/-}$ mice. Related to Figure 4. (A) Transcription factor expression profile of sort-purified $CD45^{+}$, $Gr-1^{neg}$, $F4/80^{neg}$, $CD90^{+}$, $CD127^{+}$ cells from $Rag1^{-/-}$ mice. Reconstitution of ILC compartment in the **(B)** spleen and **(C)** small intestine Lp of recipient $Rag\gamma c^{-/-}$ mice three weeks after ILC transfer.

Figure S5

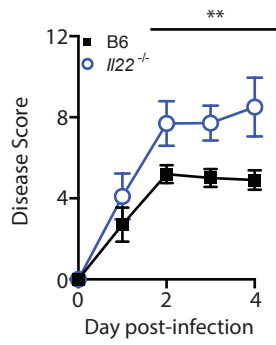
A



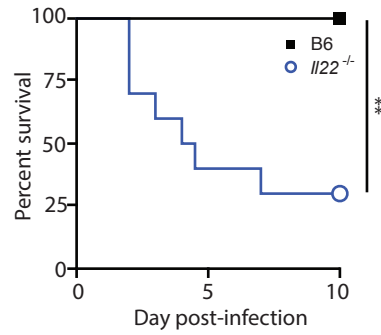
B



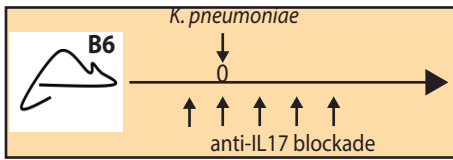
C



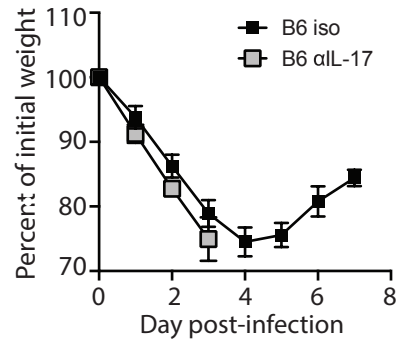
D



E



F



G

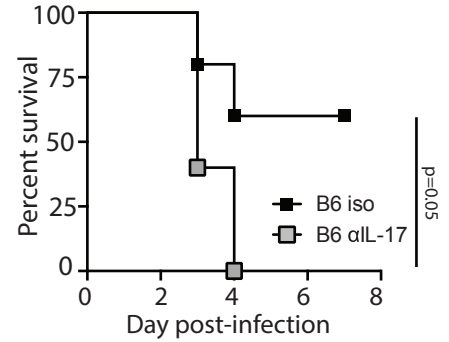


Figure S5. *Il22*^{-/-} mice exhibit increased susceptibility following six antibiotic cocktail regimen and infection with cultured inoculum of *C. difficile* bacilli. Related to Figure 5. (A) Co-housing, antibiotic pretreatment regimen and infectious dose for C57BL/6 and *Il22*^{-/-} mice. **(B)** Quantification of vegetative cells and spores in cultured inoculum. After inoculation of C57BL/6 and *Il22*^{-/-} mice, aliquots of cultured inoculum were either heat-killed at 60 °C for twenty minutes or kept at room temperature then cultured overnight in the presence or absence of the germinate taurocholic acid (TA). CFUs were compared to a pure spore inoculum. **(C)** Disease severity and **(D)** survival curve following infection. Combination of 3 independent experiments with n=10 mice per group. **(E)** C57BL/6 mice were administered with anti-IL17 neutralizing antibody or isotype control, at a dose of 500µg i.p., 200µg i.v. and 200µg intratracheal (i.t.) once a day, starting from 1 day prior to infection. Mice were then infected with 1x10³ CFU of *Klebsiella pneumoniae* (strain ATCC43816) i.t. **(F)** Weight loss and **(G)** survival following infection. n=5 each group. **p<0.01. Data shown are mean ± SEM.

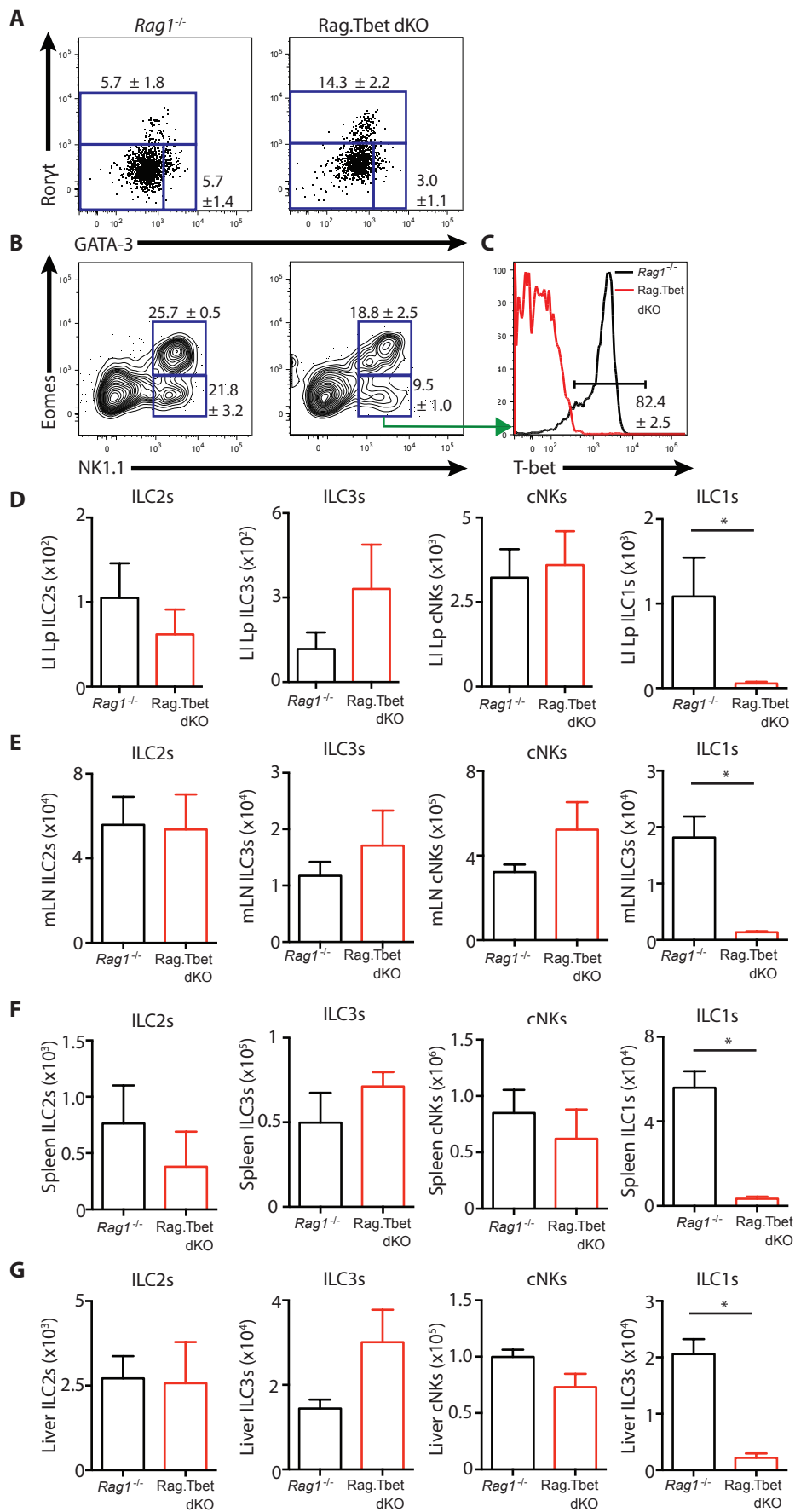
Figure S6

Figure S6. Rag.Tbet dKO mice lack ILC1s, but have comparable numbers of other subsets of ILCs. Related to Figure 6. (A-B) Transcription factor profile of ILC subsets in the large intestine Lp of naive *Rag1*^{-/-} or Rag.Tbet dKO mice. **(A)** Frequency of ROR γ t-expressing ILC3s and GATA-3-expressing ILC2s. FACS plots gated on live, CD45⁺, Gr-1^{neg}, CD90⁺, CD127⁺ cells. **(B)** Frequency of NK1.1⁺ Eomes⁺ classical NK cells and NK1.1⁺ Eomes^{neg} 'ILC1s'. FACS plots gated on live, CD45⁺, Gr-1^{neg} cells. **(C)** T-bet expression in NK1.1⁺ Eomes^{neg} cells. **(D-G)** Number of live, CD45⁺, Gr-1^{neg} NK1.1⁺, Eomes⁺ (cNKs) cells, NK1.1⁺ Eomes^{neg} 'ILC1s', CD90⁺, CD127⁺, ROR γ t-expressing ILC3s, and CD90⁺, CD127⁺, GATA-3-expressing ILC2s, in the **(D)** large intestine Lp, **(E)** mLN, **(F)** spleen, and **(G)** liver of *Rag1*^{-/-} or Rag.Tbet dKO mice. Data representative of 3 independent experiments. n=3-4 mice per group. *p<0.05. Data shown are mean \pm SEM.

Supplemental Experimental Procedures

Quantification of *C. difficile* burden and toxin

Fecal pellets or cecal content were resuspended in deoxygenated phosphate-buffered saline (PBS), and ten fold dilutions were plated on BHI agar supplemented with yeast extract, taurocholate, L-cysteine, cycloserine and ceftiofur at 37°C in an anaerobic chamber (Coylabs) overnight. (Sorg and Dineen, 2009). The presence of *C. difficile* toxins was determined using a cell-based cytotoxicity assay as previously described (Jarchum et al., 2011). Briefly, human embryonic lung fibroblast WI-38 cells (ATCC# CCL-75) were incubated in a 96-well plate overnight at 37°C. Ten fold dilutions of supernatant from resuspended cecal content was added to WI-38 cells, incubated overnight at 37°C and the presence of cell rounding and death was observed the next day. The presence of *C. difficile* toxins A and B was confirmed by neutralization by antitoxin antisera (Techlab, Blacksburg, VA). The data are expressed as the log₁₀ reciprocal value of the last dilution where cell rounding was observed.

Bacterial DNA extraction, amplification and analysis

DNA was extracted from fecal pellet as previously described in (Ubeda et al., 2012), and 16S rRNA genes were amplified by PCR. Amplicons of the V4-V5 16S rRNA region were amplified and sequenced using an Illumina MiSeq platform as described in Buffie et al., 2015. Sequencing data was analyzed and processed using the MOTHUR pipeline (Schloss et al., 2009). Operational taxonomical units (OTU) were classified using the modified Greengenes database. A phylogenetic tree was inferred using Clearcut on the 16s rRNA sequence alignment generated by MOTHUR (Sheneman et al., 2006). Weighted UniFrac was run using the resulting tree, and principal component analysis was performed on the resulting matrix of distances between each pair of samples (Ubeda et al., 2012).

Assessment of bacterial translocation

Cecal supernatants were assessed for albumin levels by ELISA (Bethyl Labs). Serum was isolated from blood by clotting sample on ice for four hours then centrifuging at 14,000 rpm for thirty minutes. LPS levels in serum were determined by Limulus Amebocyte Lysate chromogenic endotoxin quantification kit (Pierce Labs). The fluorescence *in situ* hybridization method was adapted from (Swidsinski et al., 2005; Vaishnava et al., 2011). Sections were incubated with a universal bacterial probe directed against the 16S rRNA gene (EUB338: [Cy3]-GCTGCCTCCCGTAGGAGT-[AmC7~Q+Cy3es] and counterstained with Hoechst for nuclear staining. Images were acquired with a Leica TCS SP5-II upright confocal microscope using a 20x or 63x oil immersion lens (NA 1.4, HCX PL APO) as a series of short Z-stacks. Maximum intensity projection processing of Z-stacks was done in Fiji (ImageJ) software.

Isolation of cells from spleen, lymph nodes and intestine

Lymphocytes were isolated from the spleen or lymph node by mechanical disruption through 100 μ m cell strainers followed by red blood cell lysis. Single cell suspensions were obtained from the large intestine intraepithelial lymphocyte (IEL) compartment and lamina propria (Lp) by longitudinally cutting the large intestine then washing out content in PBS. Intestinal tissues were incubated at 37°C under gentle agitation in stripping buffer (PBS, 5 mM EDTA, 1 mM dithiothreitol, 4% FCS, 10 μ g/mL penicillin/streptomycin) for 10 minutes to remove epithelial cells then for another 20 minutes for the IEL. Supernatants containing the IEL fraction were passed through 100 μ m cell strainers and resuspended in 40% Percoll. The remaining tissue was digested with collagenase IV 1.5 mg/mL (500 U/mL), DNase 20 μ g/mL in complete media (DMEM supplemented w/ 10% FBS, 10 μ g/mL penicillin/streptomycin, 50 μ g/mL gentamicin, 10 mM HEPES, 0.5 mM β -mercaptoethanol, 20 μ g/mL L-glutamine) for 30 minutes at 37°C under gentle agitation. Supernatants containing the Lp fraction were passed through a 100 μ m cell

strainers and resuspended in 40% Percoll. Samples were then centrifuged for 20 minutes at 600x g to obtain IEL and Lp cell fractions.

Ex vivo cytokine detection and flow cytometry

For direct *ex vivo* cytokine detection, cells isolated Following incubation, cells were surface stained in FACS Buffer (PBS, 2% BSA, 0.2 mg Sodium Azide, 2 mM EDTA) using standard flow cytometric staining protocol with fluorescently conjugated antibodies specific to CD3 ϵ , CD4, CD5, CD8 α , CD19, CD45, CD90, CD127, Gr-1 (clone RB85), $\gamma\delta$ TCR, NKp46 (eBioscience), and NK1.1 (Biolegend). After staining for surface antigens, cells were stained for intracellular cytokines using intracellular cytokine fixation buffer (eBioscience) and fluorescently conjugated antibodies specific for IL-22 (clone 1H8PWSR, eBioscience), IFN- γ (clone XMG1.2 BD Biosciences), Cell viability was assessed with Live/Dead AQUA stain (Invitrogen). For intranuclear staining, the transcription factor staining kit (eBioscience) was used and cells stained with fluorescently conjugated antibodies specific for T-bet (clone eBIO4B10), GATA-3 (clone TWAJ), ROR γ t (clone B2D), and Eomes (clone DAN11MA6) Samples were collected by using a LSR II flow cytometer (Becton Dickinson). All flow cytometry data was analyzed by FlowJo v 9.7 (Treestar).

Cecal tissue explant

Cecum was cut open longitudinally and washed in PBS. Tissue samples were incubated overnight in complete media. Following incubation, tissue samples were weighed and supernatants were assessed for IFN- γ (BD OptiEIA) and IL-22 (Antigenix). protein by ELISA.

Supplemental References

- Jarchum, I., Liu, M., Lipuma, L., and Pamer, E.G. (2011). Toll-like receptor 5 stimulation protects mice from acute *Clostridium difficile* colitis. *Infection and immunity* 79, 1498-1503.
- Schloss, P.D., Westcott, S.L., Ryabin, T., Hall, J.R., Hartmann, M., Hollister, E.B., Lesniewski, R.A., Oakley, B.B., Parks, D.H., Robinson, C.J., *et al.* (2009). Introducing mothur: open-source, platform-independent, community-supported software for describing and comparing microbial communities. *Applied and environmental microbiology* 75, 7537-7541.
- Sheneman, L., Evans, J., and Foster, J.A. (2006). Clearcut: a fast implementation of relaxed neighbor joining. *Bioinformatics* 22, 2823-2824.
- Sorg, J.A., and Dineen, S.S. (2009). Laboratory maintenance of *Clostridium difficile*. *Curr Protoc Microbiol Chapter 9, Unit9A 1*.
- Swidsinski, A., Loening-Baucke, V., Lochs, H., and Hale, L.P. (2005). Spatial organization of bacterial flora in normal and inflamed intestine: a fluorescence in situ hybridization study in mice. *World J Gastroenterol* 11, 1131-1140.
- Ubeda, C., Lipuma, L., Gobourne, A., Viale, A., Leiner, I., Equinda, M., Khanin, R., and Pamer, E.G. (2012). Familial transmission rather than defective innate immunity shapes the distinct intestinal microbiota of TLR-deficient mice. *The Journal of experimental medicine* 209, 1445-1456.
- Vaishnava, S., Yamamoto, M., Severson, K.M., Ruhn, K.A., Yu, X., Koren, O., Ley, R., Wakeland, E.K., and Hooper, L.V. (2011). The antibacterial lectin RegIIIgamma promotes the spatial segregation of microbiota and host in the intestine. *Science* 334, 255-258.